Fermi Level Alignment and Electronic Levels in "Molecular Wire" Self-Assembled Monolayers on Au

C. D. Zangmeister, S. W. Robey,* and R. D. van Zee

National Institute of Standards and Technology, Gaithersburg, Maryland 20899

Y. Yao and J. M. Tour

Department of Chemistry and Center for Nanoscale Science and Technology, Rice University, Houston, Texas 77005

Received: April 29, 2004; In Final Form: July 23, 2004

One- and two-photon photoelectron spectroscopies were used to determine the electronic structure around the Fermi level for self-assembled monolayers of a prototypical "molecular wire", 4,4′-(ethynylphenyl)-1-benzenethiol ($C_6H_5-C\equiv C-C_6H_4-C\equiv C-C_6H_5-SH$), on Au. One−photon ultraviolet photoelectron spectroscopy indicated a separation between the Fermi level and the peak of the occupied delocalized π levels of 1.9 eV, thus providing a representative value for the hole injection barrier. Two states were identified in two-photon photoelectron spectroscopy measurements corresponding to excitation to the lowest exciton and excitation to an unoccupied final state derived from the e_{2u} levels of benzene. The separation between the Fermi level and the corresponding unoccupied π^* states is estimated to be 3.2 eV, giving a transport gap of $\sim 1.9 + 3.2 = 5.1$ eV. Occupied states associated with Au−S interactions are observed near the Fermi level for comparison studies on benzenethiol monolayers. Charge transfer associated with the formation of these levels, and their unoccupied counterparts, is suggested to produce the approximately 0.7 eV shift of the Fermi level toward the highest occupied orbitals on the oligomer.

Introduction

Successful utilization of conjugated molecular systems in electronic applications, in either the guise of thin films for organic light emitting diodes (OLEDs) or field-effect transistors or more speculative applications proposed for molecular electronics, requires understanding of the molecular electronic structure including modifications occurring due to coupling to electrodes. Identifying molecular levels, occupied and unoccupied, available for transport in the molecule and determining barriers to hole or electron injection from metallic contacts into these levels are features of particular interest that will dominate charge injection and transport behavior in organic device applications. This information is available from a variety of techniques, including transport or optical measurements, but photoelectron spectroscopy-related methods provide perhaps the most direct means of investigating the molecule−contact interface. One-photon photoelectron spectroscopy provides direct access to the energies and characteristics of the occupied electronic levels[1] while either inverse photoemission measurements[2] or two-photon photoelectron spectroscopy[3] allows investigation of unoccupied levels.

Stimulated by reports of novel transport behavior in molecular systems based on phenylene−ethynylene oligomers,[4] and the resulting theoretical efforts to explain these effects,[5] we have employed ultraviolet photoelectron spectroscopy (UPS) to provide a picture of the electronic structure for self-assembled monolayers of 4,4′-(ethynylphenyl)-1-benzenethiol ($C_6H_5-C\equiv C-C_6H_4-C\equiv C-C_6H_4-SH$) on gold. A schematic representation of the molecule adsorbed on Au is provided in Figure. 1. Variants of this molecule have been the subject of intense interest associated with reports of negative differential resistance in nanoscale junctions upon substitution of NO_2 on the central ring.[4]

The major motivation for this work is to provide a picture of the location and characteristics of the molecular orbitals for this oligomer, particularly for the π-based levels involved in transport across the molecule. The placement of these levels relative to the Au Fermi level will determine the efficacy of charge injection into the molecule. Also of interest will be similarities and differences in the electronic structure of related conjugated polymers systems and small organic molecules studied in the context of OLEDs or other electronic applications.[6] The self-assembled systems studied here differ from the those systems because of the thiol linkage to the substrate. Determining the influence of this coupling on band lineup, in comparison with analogous polymers such as para-(phenylene−vinylene) (PPV), is an additional goal of this study. Overall, this work provides direct spectroscopic information on the electronic structure and barrier formation for 4,4′-(ethynylphenyl)-1-benzenethiol and should furnish much needed benchmarks for evaluating theoretical treatments of transport behavior in OPE and related systems.

Experimental Section

Sample Preparation. The oligo-(phenylene−ethynylene) compound was synthesized as reported previously.[7] Ethanol (Warner-Graham Co., 200 proof)[8] was distilled over magnesium shavings (Aldrich Chemical) in a nitrogen atmosphere. Tetrahydrofuran (THF, Aldrich)[8] and dichloromethane (CH_2Cl_2, Aldrich)[8] were distilled over calcium hydride. All distillations were preformed in a N_2 atmosphere. Ammonium hydroxide (Aldrich, 30% NH_4OH in H_2O)[8] was used as received.

10.1021/jp048134c CCC: $27.50
Published on Web 09/18/2004

Monolayers were grown on Au (111)/mica (Molecular Imaging)[8] and polycrystalline gold surfaces. Some experiments were also performed on single-crystal Au(111) surfaces prepared by repeated cycles of sputtering and annealing. The polycrystalline Au films were prepared by evaporation of 200 nm of Au on a 20 nm Cr adhesion layer onto a nonheated Si (100) substrate. All Au films were cleaned prior to SAM formation by exposure to UV/O_3 for 15 min followed by rinsing for 30 s with 18.2 MΩ H_2O and blown dry with a stream of ultrapure N_2. Reflection absorption infrared spectroscopy (RAIRS) characterization was performed for SAMs on polycrystalline substrates, grown concurrently with SAMs produced for photoemission measurements, to ensure monolayer quality.

All SAM formation was performed in an argon-purged glovebox with an O_2 concentration <1 ppm. Monolayers were grown in covered glassware to prevent possible decomposition due to light exposure. SAMs of 4,4′-(ethynylphenyl)-1-benzenethiol (OPE) were prepared by dissolution of the solid into 20 mL of CH_2Cl_2 followed by addition of 10 mL of ethanol to form a ∼0.5 mM solution. Gold substrates were added to the solution after complete dissolution, and the vial was sealed for the requisite exposure time (∼24 h) in the argon-purged environment. SAMs of benzenethiol were grown in a 1 mM solution of distilled ethanol for 24 h in an argon-purged drybox. The substrates were rinsed in the drybox with CH_2Cl_2 after removal from solution. RAIRS, contact angle, and scanning ellipsometry data were acquired on samples grown concurrently with those used in the UPS investigation to ensure monolayer quality and were consistent with those of previous reports of each of the monolayers.

SAMs on Au/mica were mounted on the sample manipulator and loaded into the analysis chamber fast entry lock immediately after rinsing with solvent. The sample was moved from the fast entry lock into the analysis chamber after ∼3 h. The analysis chamber maintained an operating pressure of 2×10^{-10} mbar during the course of the experiments.

Core-level photoelectron spectroscopy measurements were performed in both the UPS measurement chamber, using nonmonochromatic Al Kα radiation, and a separate analysis system that afforded the capability of employing monochromatic Al Kα excitation. Oxygen was the only identifiable contaminant, typically at ∼1 to 2% atomic concentration, with levels as high as 5% in some samples. Changes in the measured oxygen content from monolayer to monolayer had no discernible influence on the measured UPS spectra. Also, no evidence of oxidation was observed in the S 2p core level. Intentional increases in the atmospheric exposure produced an overall reduction and broadening of the valence electronic structure, but no significant shifting of peak positions. Spectra could be restored by annealing to ∼500 K (230 °C). These results and the strong similarity to photoelectron spectra obtained from high-quality, contamination-free PPV films (see below) suggest that the residual oxygen content does not influence the spectroscopic assignment of the features given below.

No correlation was observed between the Fermi level position and oxygen content, although the available variation in oxygen content was small. In related studies[9] we have demonstrated that substitution of isocyanide for thiol as the surface linkage produces a large shift of the Fermi level position within the molecular gap. This would not be possible if the oxygen, or other impurities, present in the monolayers played a dominant role in pinning the Fermi level.

Ultraviolet Photoelectron Spectroscopy. Ultraviolet photoelectron spectra were obtained with excitation via a linearly polarized He I (21.2 eV) line source equipped with a three-mirror polarizer. The light was incident at 45° from the sample normal, and photoelectrons were collected at normal emission with a 180° hemispherical electrostatic analyzer. The analyzer was operated at 3 eV pass energy, providing a typical resolution of about 100 meV. Two polarization configurations were employed to assess molecular orientation effects. Aligning the polarization perpendicular to the plane of incidence produced s-polarization (electric vector purely in the sample surface plane) while rotating it parallel to the light/detector plane resulted in an equal mixture of s- and p-polarization.

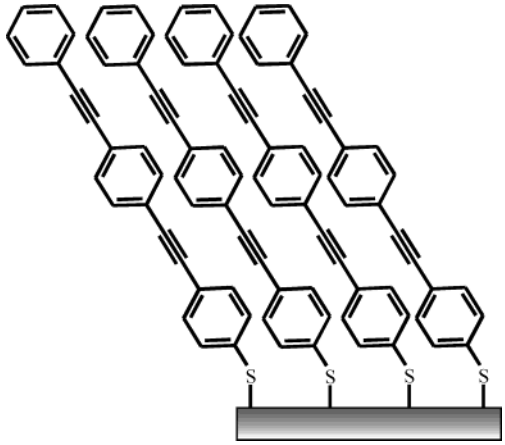

Figure 1. Schematic illustration of the molecular structure for 4,4′-(ethynylphenyl)-1-benzenethiol (OPE).

Two-Photon Photoelectron Spectroscopy. Information on the unoccupied levels in the OPE monolayer was provided by two-photon photoelectron spectroscopy measurements, employing the same 180° electrostatic analyzer. Excitation was via the frequency-doubled output of a Ti:sapphire pumped optical parametric amplifier (tunable from about 3.2 to 4.5 eV, pulse duration ≈ 0.1 ps, 2 mW in ∼0.6 mm^2 at sample, repetition rate = 0.25 MHz). Photons were incident at 45° to the sample surface, polarized in the plane of incidence, and photoemitted electrons were collected at normal emission typically with a −5 V bias on the sample.

Results

One-Photon Spectra. Representative ultraviolet photoelectron spectroscopy data from a monolayer film of OPE molecule are displayed in Figure 2. The spectra are dominated by three broad peak structures at binding energies, referenced to the Au Fermi level (E_F), with maxima at 3.8, 6.5, and 9.0 eV. (In the following discussion, binding energies will be referenced as positive for occupied states below the Fermi level.) Peak broadening dominates the uncertainty in locating peak positions, typically ∼±0.1 eV for a reasonably well-defined peak. Other effects such as analyzer energy scale or excitation energy uncertainties contribute at a negligible level.

The sample work function was measured using the low kinetic energy threshold in the spectrum, typically with a bias applied to the sample of between −1 and −5 V. Values for clean gold varied between 4.9 and 5.1 eV, depending on whether the substrate was polycrystalline Au on Si, Au on mica, or single-crystal Au (111). Adsorption of the OPE monolayer lowered the work function to 4.2 eV.

Photoemission intensity from the underlying Au substrate was estimated by scaling a clean gold spectrum to the remnant intensity at the Fermi edge in the OPE spectrum. The substrate contribution was typically less than 20% throughout the

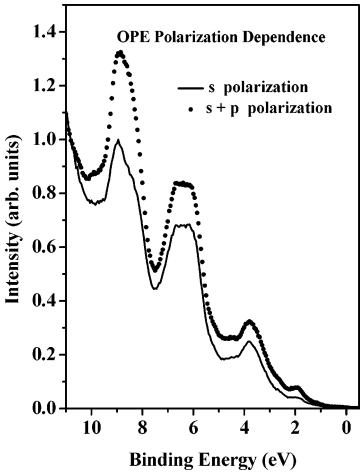

Figure 2. UPS spectra (21.2 eV excitation) for a monolayer of thiol-bound OPE on Au. Spectra taken with s polarization (line) are compared with spectra for s + p polarization (solid squares).

spectrum, so the UPS data in Figure 2 are dominated by the molecular electronic structure of the OPE. Spectra from OPE monolayers on all three substrates—polycrystalline Au/Si−Au-(111) on mica, and single-crystal Au(111)—were basically identical. Because there are significant differences in the Au spectra from polycrystalline versus single crystal substrates this is also an indication that the substrate intensity does not significantly perturb spectra from the thiol-bound oligomer.

Spectra for gas phase[10] or adsorbed multilayers[11] of benzene consist of three main bands quite similar to the features observed for OPE. This similarity suggests considering C_6H_6 as a starting point for interpreting the spectra from OPE. Using the measured work function of 4.2 eV for the OPE monolayer, experimental ionization energies of the three main bands in the gas phase spectrum can be compared with corresponding ionization energies for structure in the OPE monolayer. An approximately rigid shift of ∼1.1 eV, to lower binding energy, is found for all of the peaks in the adsorbed monolayer. This shift arises from increased final state screening for the adsorbed monolayer, including intramolecular and intermolecular contributions within the monolayer and screening due to the Au substrate. This value for the relaxation shift is consistent with those typically observed for polymers and molecular solids.[12]

With these adjustments, features in the OPE spectra in Figure 2 can be associated with the corresponding bands in benzene.[10,11] The intensity at about 9 eV is associated with a combination of σ-like b_{1u} and b_{2u} states on the high binding energy side and e_{1u} states on the lower energy side. The next band at ∼6.5 eV is composed of a_{2u} orbitals at high binding energy and e_{2g} orbitals closer to E_F. The third band in benzene, associated with structure around 3.8 eV in the monolayer, arises from the e_{1g} π orbitals. Following these associations, the levels in OPE can be divided into a predominantly σ-bonding region for binding energies above ∼5 eV and predominantly π-bonding states below.

This orbital description is modified by coupling, by ethynlene groups, between phenylene rings in the oligomer. The most prominent effect occurs in the π-bonding region where the peak at 3.8 eV, associated with the lowest binding energy band in benzene, has additional weak, broad structure to either side at around 1.9 and 4.5 eV. The coupling breaks the degeneracy in doubly degenerate e_{1g} orbitals of benzene. One e_{1g} orbital has significant density on the para-carbon atoms, while the other is predominantly localized on the ortho-carbon atom, with negligible weight at the para-positions. Interaction of the out-of-plane π orbitals of the C≡C bond between rings with e_{1g} orbital on the para-carbons produces bonding and antibonding intensity at ∼4.5 and ∼1.9 eV, respectively. The e_{1g} level confined to the ortho-carbon atoms remains relatively localized on the ring providing intensity in the peak at 3.8 eV. This is analogous to the interpretation of UPS spectra for conjugated polymers such as PPV provided by electronic structure calculations, where the lowest binding energy π band is composed of e_{1g}-derived levels delocalized along the polymer backbone while the next lowest binding energy peak arises from the localized ortho-carbon orbitals, forming an essentially flat band.[13] The strong similarity between UPS data for high-quality PPV films and the OPE data confirms this interpretation.

The polarization dependence displayed in Figure 2 can provide information on molecular orientation of the monolayer. A detailed consideration is complicated by molecular tilt away from normal, suggested by RAIRS measurements,[14] and multiple orientations of domains in the monolayer and polycrystalline substrate. However, a simple discussion, concentrating on the predominantly C−C and C−H bonding orbitals at higher binding energy, should allow a qualitative determination of whether the molecule is predominantly upright or parallel to the substrate surface. These σ levels remain qualitatively similar to their counterparts for an isolated benzene molecule, suggesting consideration of two simple, limiting cases—C_{2v} molecules either parallel or perpendicular to the surface.

When the ring plane is parallel to the surface, the benzene b_{1u}, b_{2u}, and e_{1u} orbitals contributing to the 9 eV peak acquire b_1 and b_2 symmetry while the a_{2u} and e_{2g} states near 6.5 eV produce a_1 and a_2 orbitals. For photoelectron detection at normal emission, b_1 and b_2 symmetries are allowed with s-polarization, but the intensity is zero for p-polarized radiation. The opposite is true for the a_1 and a_2 symmetries around 6.5 eV, i.e., no intensity with s-polarization and finite intensity for p-polarization. This leads to the expectation that the ratio of the intensity at 9 eV to that at 6.5 eV should decrease with increasing p-polarized content. However, Figure 2 shows significant intensity at 6.5 eV for s-polarization at 9 eV for p-polarization with possibly a slight increase in the intensity ratio, $I_{9\,eV}/I_{6.5\,eV}$, with the addition of the p-polarized component, contrary to expectation. In contrast, with the ring plane perpendicular to the surface, the b_1, b_2, and e_{1u} components at 9 eV produce a_1 and b_2 symmetry orbitals. Again, the a_1 state is allowed for p-polarization while the b_2 is preferentially excited with s-polarization. The e_{2g} and a_{2u} states at ∼6.5 eV also produce a similar mix of b_2 and a_1 symmetry. Qualitatively, both bands should be allowed for normal emission, and there should be only relatively small intensity changes as the polarization is varied. This scenario more closely matches the observed weak polarization dependence, suggesting that the molecular orientation is best described with the phenylene plane close to perpendicular to the Au surface as determined with RAIRS.[14]

Thiolate−Au Interaction. The thiol−Au bond is expected to play an important role in determining the band lineup and the providing coupling from Au levels near E_F into the π levels on the molecule.[15] Obtaining a clear picture of the bonding interaction from photoemission spectra for OPE is hampered, however, by electron attenuation in the ∼2 nm thick oligomer monlayer. Sulfur contributions at the Au−molecule interface are substantially weakened by and masked by intensity from the carbon π orbitals. Some information, at least at a qualitative level, can be provided by investigations of the Au−S bonding in shorter thiol-bound SAMs. Benzenethiol adsorbed on Au and Cu has been studied previously,[16] and those results have

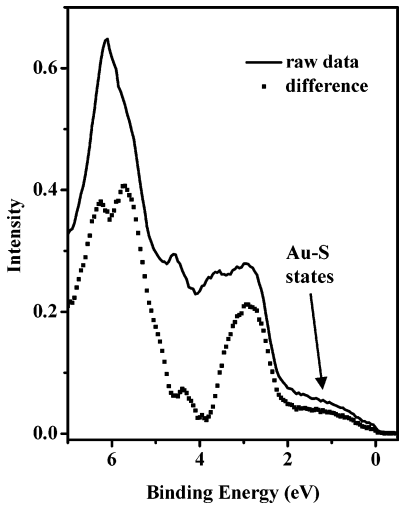

Figure 3. UPS spectrum from a monlayer of benzenethiol on Au. The solid line provides the raw data, and the solid squares provide a difference curve produced by subtracting the intensity in a clean Au spectrum after normalizing to the raw data at the Fermi level.

provided a reasonable description of the S−Au interaction, although strong Au or Cu d-band contributions from the substrate continue to interfere with the ability to obtain detailed information.

A typical UPS spectrum for the low binding energy region for a benzenethiol monolayer is displayed in Figure 3. Both the raw data and a difference spectrum obtained by subtracting a clean Au spectrum after normalizing at E_F are provided. The general features agree quite well with previous studies.[16] The weak, broad intensity just below the Fermi level, centered at ~1 eV, corresponds well with structure observed for S monolayers on metals[17] and for alkanethiol monolayers.[18] Theoretical results suggest that intensity in this spectral region is derived from antibonding contributions from the Au−S interaction, localized at the S−Au interface.[19] The absence of observable structure in this region for the longer OPE molecule, due to electron attenuation in the monolayer, supports the suggestion that these levels are localized near the Au−molecule interface while the observation of similar structure for saturated alkanethiol monolayers indicates that interaction with the organic portion of the molecule plays a limited role in the Au−S interaction that produces these levels.

Two-Photon Photoelectron Spectra. Two-photon photoemission measurements were performed to provide information on unoccupied levels. These experiments are reported elsewhere,[20] and only a brief description will be provided here. Two-photon excitation of OPE monolayers in the photon energy range from about 3.2 to 4.2 eV produced spectra with one feature fixed at about 0.9−1.0 eV above the vacuum level and another weaker feature closer to the Fermi level for these excitation energies. Neither of these features was observed in two-photon measurements for saturated decanethiol monolayers.

Figure 4a presents a representative 2PPES spectrum, with excitation at $h\nu = 3.86$ eV, after background subtraction. The two peaks noted above are observed at kinetic energies of 5.1 ± 0.1 and 6.4 ± 0.1 eV. The measured kinetic energy as a function of $h\nu$ for each of these structures is plotted in Figure 4b. This dependence on excitation energy allows determination of the origin of the level as either an occupied initial state, an unoccupied intermediate state, or an unoccupied final state.[21] The expected two times the $h\nu$ dependence observed for coherent two-photon transitions from fixed (occupied) initial states at the Fermi level is included as a consistency check.

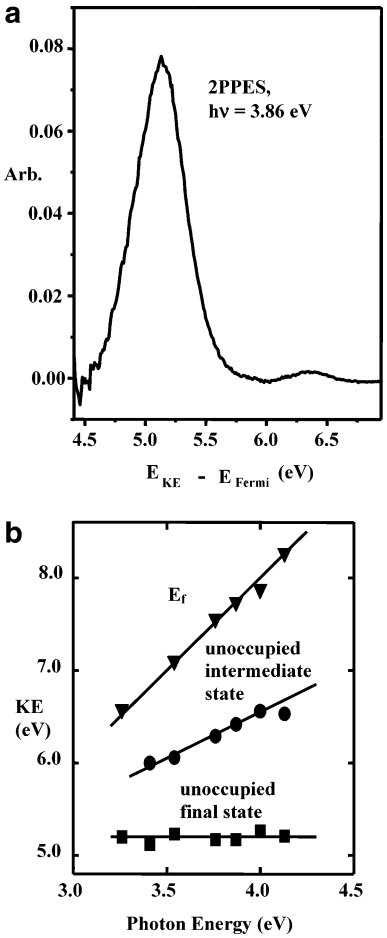

Figure 4. (a) Representative 2PPES spectrum, at an excitation energy of 3.86 eV, for a monolayer of OPE on Au. (b) Plots of the dependence of the final kinetic energy (above E_f) versus the excitation energy for the two structures observed in 2PPES from OPE. (Note that, in accordance with our convention, binding energies for these levels would be the negative of the $E_{KE} - E_f$ values.) The $h\nu$ dependence of the occupied states near Fermi level is also shown to illustrate dispersion in the case of excitation of an initially occupied state. The $1 \times h\nu$ dependence observed for one of the 2PPES features allows it to be associated with an unoccupied intermediate state while the other exhibits no dispersion with excitation energy, indicating a 2PPES process to an unoccupied final state above the vacuum level. These features are further assigned to the lowest exciton and the unoccupied π^* levels, respectively (see text).

The weaker feature, at 6.4 eV in Figure 4a, exhibits a dependence on the excitation energy of about one times $h\nu$, indicating it arises by transient population of an unoccupied intermediate state 2.5 eV ± 0.1 above the Fermi level or 1.7 eV ± 0.1 below the vacuum level. The separation between this level and the occupied π level 1.9 eV below E_F is then about 4.4 ± 0.15 eV. This coincides with the optical absorption maximum for OPE monolayers.[22] The intensity dependence also seems to track the OPE absorption reasonably well, although the low intensity of this peak and the limited excitation range available make a definitive statement impossible. These factors suggest that the intermediate state populated during the two-photon process is the lowest singlet exciton level observed as the leading edge of the optical absorption.

The absence of any photon energy dependence for the second peak in the 2PPES spectra indicates transitions to an unoccupied final state located about 5.2 ± 0.1 eV above the Fermi level. Results from previous two-photon photoemission and inverse photoemission measurements for condensed layers of benzene/Cu (111)[21] and benzene on Au (110),[23] along with secondary

electron transmission spectroscopy (SETS) studies of Langmuir−Blodgett films produced from phenyl-ring containing molecules,[24] suggest that this level should be attributed to the formation of a temporary negative ion resonance ($N + 1$ electron level) of the benzene-derived e_{2u} unoccupied level that is the counterpart of the occupied e_{1g} level observed at 3.9 eV in UPS. As in the case of the occupied e_{1g} orbitals, the unoccupied e_{2u} orbital in benzene is doubly degenerate. The orbital localized predominantly on the ortho-carbon atoms of the phenylene rings gives rise to the observed structure at 5.2 eV above E_F. The unoccupied level corresponding to the occupied delocalized π level observed at 1.9 eV most likely cannot be observed as negative ion resonance because it is located below the vacuum level. The close correspondence with SETS measurements[24] suggests population of these negative ion resonances occurs via capture of hot electrons produced by Au optical absorption.

Fermi Level Alignment. A major motivation for this work was determination of the alignment of the Au Fermi level in the gap between the molecular HOMO and LUMO levels that determines injection of charge into molecular levels. The separation between E_F and the occupied levels can be determined directly from UPS while additional data from optical absorption, inverse photoemission, or two-photon photoemission studies is needed to access the location of unoccupied levels that control electron injection into the molecule.

Identification of positions in the UPS spectra that can be quantitatively associated with hole or electron injection barriers determined, for instance, via transport measurements, is not straightforward. Defining molecular HOMO and LUMO levels for the coupled molecule−Au system is ambiguous, and the importance of a particular orbital in determining transport properties of the molecular scale junction depends on the separation from the Fermi level and the degree of delocalization across the junction.[25] Au−S bonding produces levels in close proximity (∼1 eV) to the Fermi level but which are localized to the interface with limited extent into the molecular gap. On the other hand, occupied π levels at −1.9 eV, and their unoccupied counterparts, are more delocalized along the oligomer but substantially further removed from the Fermi level. Identifying which of these may dominate in determining electron or hole "injection barriers", and what those barriers will be is not clear.[25] Broadening in the UPS spectra leads to additional uncertainty. The broadened features could arise from a variety of sources, including inhomogeneous molecular environments, delocalization due to intra- and intermolecular coupling and substrate coupling, vibrational structure, and variations in final state screening. The predominant source of broadening, if any, determines whether peak or threshold positions are most appropriate in evaluating injection. Finally, the photoemission measurements, because of electron attenuation, do not necessarily provide an evenly weighted picture of the molecular density of states for the 2.0 nm long oligomers studied here. Interface-localized perturbations associated with the Au−S− oligomer bond will be less visible in the photoemission spectra.

The "injection barriers" resulting from the Fermi level lineup in the molecular gap will be defined below simply as the separation between the Fermi level and the peak positions of the occupied and unoccupied levels arising from delocalized π orbitals on the oligomer. These orbitals are expected to provide the most efficient resonant coupling across the molecule in the limit of a long oligomer. However, these values should not be construed as having a simple quantitative connection to barriers determined from model fits to transport data in molecular scale junctions.

An expanded view of the binding energy region near the Fermi level is provided in Figure 3, including the region from the Fermi level to above the first peak in the density of states that has been assigned above to molecular π levels delocalized along the oligomer backbone. From the discussion above, the hole injection barrier is given by the peak-to-Fermi level separation of 1.9 ± 0.1 eV. Incomplete relaxation of the hole state created during the photoemission measurement could cause this to be an overestimation of this actual separation, but the estimated relaxation energy of ∼1.1 eV and the extended nature of the π levels suggest this effect would be small.

Additional information is required for an estimate of an electron injection barrier. One possibility involves using the optical absorption peak measured for OPE monolayers on Au at ∼4.35 eV.[22] The lowest optical transition to a polaron−exiton state differs from the charge transport gap by the polaron−exciton binding energy. Values for the exciton binding energy between 0.6 and 1.4 eV were determined for a number π-conjugated organic thin films using UPS and IPES.[2,26] Assuming an average value of ∼1.0 eV produces an estimate of the expected peak-to-peak HOMO−LUMO separation (separation in the $N - 1$ to $N + 1$ spectra that one would find in, for instance, a combination UPS/IPES measurement) of 4.3 eV (optical absorption gap) + 1.0 eV (estimated polaron-exciton binding energy) ∼ 5.3 eV (transport gap). Subtracting the HOMO peak-to-Fermi level separation measured in UPS then provides an estimate for the location of the LUMO ($N + 1$) peak at about 5.3 eV − 1.9 eV = 3.4 eV above the Fermi level. This value represents the barrier to injection from the Fermi level into the peak of the unoccupied molecular π levels extending across molecule (electron injection barrier).

2PPES measurements allow an additional estimate for the location of the delocalized π^*, or $N + 1$ polaron state, that requires an assumption about the splitting between the localized π^* levels, measured at 5.2 eV above E_F, and delocalized π^* levels. The necessity for this assumption arises because the electron−polaron state ($N + 1$) associated with the π^* levels cannot be observed directly, as mentioned previously. On the basis of simple bonding arguments and semiempirical electronic structure calculations for analogous polymer systems,[27] it is assumed that the splitting in the unoccupied levels is close to the splitting of about 2 eV measured for the occupied levels in one-photon photoemission. This also seem to be a quite reasonable assumption based on measured splittings in combination UPS/IPES measurements for anthracene.[28] The delocalized π^* orbitals are then estimated to lie approximately 5.2 ± 0.1 eV (position of the "localized" unoccupied level) − 2.0 ± 0.1 eV = 3.2 ± 0.15 eV above the Fermi level. This then provides an estimate of the exciton binding energy of approximately 3.2 eV − 2.5 eV (measured position of the exciton state) = 0.7 eV, a quite reasonable value. The transport gap, defined in terms of the peak-to-peak $\pi-\pi^*$ separation, is then ∼1.9 + 3.2 = 5.1 eV, and the Fermi level is shifted approximately 0.7 eV from mid-gap toward the HOMO.

Both estimates of the HOMO−LUMO splitting involve assumptions, either for the exciton binding energy or for the splitting in the unoccupied levels. Without detailed knowledge of these values, we can only ascertain that the transport gap (peak-to-peak value) lies between the limiting values of 1.9 eV + 2.5 eV = 4.4 eV and 1.9 eV + 5.1 eV = 7 eV. However, both assumptions employed in obtaining these estimates are reasonable and lead to quantitatively consistent pictures of the unoccupied electronic structure, suggesting that the peak-to-peak separation associated with the transport gap in OPE is close

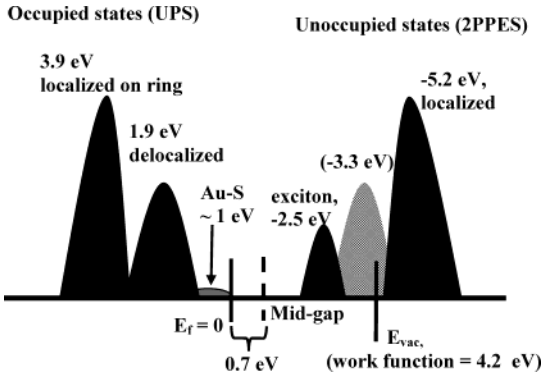

Figure 5. Schematic illustration of the electronic structure around the Fermi level for OPE monolayers, determined by the combination of one- and two-photon photoemission. The levels depicted in light gray shading represent the estimated position of the delocalized π^* levels (the $N + 1$ electron−polaron states).

to the suggested values of 5.1−5.3 eV. Further work is needed to definitively settle this question.

A complete diagram of the proposed band lineup in carbon π-orbitals is given in Figure 5. We emphasize that this diagram presents the band lineup in the zero- or low-bias limit with coupling at only one electrode. Stabilization or destabilization of orbitals on opposite sides of the junction may become important with increased bias in $I-V$ measurements in molecular junctions. In both pictures provided above, using either optical absorption plus an estimate of the exciton binding energy or the location of the localized π level from 2PPES plus an estimate of the unoccupied level splitting, the Fermi level is shifted toward the occupied levels by about 0.7 eV.

Discussion

The UPS results provided here for OPE monolayers provide useful insight into the electronic structure and coupling of the molecule to the Au substrate, with direct impact on charge transport through the molecule. The strong similarity in UPS spectra for OPE and thin films of PPV or PPV oligomers indicates that the effect of the thiol coupling is largely confined to the interfacial region and leads to limited perturbation of the molecular π system, although results for benzenethiol seem to indicate significant electronic structure modifications over the first phenyl ring. These findings are generally consistent with theoretical conclusions.[14,29]

A difference is noted, however, in the position of the Fermi level between OPE and PPV. Bredas et al. estimated that the Fermi level of Au is aligned at approximately mid-gap for thin films of PPV. This is not unexpected for an intrinsic semiconductor and is also consistent with complex band structure calculations performed for an infinite phenylene−ethynylene chain.[30]

In contrast, a shift of the Fermi level by about 0.7 eV, from mid-gap toward the HOMO, is present for thiol-bound OPE. The broad weak intensity, observed in UPS of benzenethiol, indicates that occupied states arising from Au−S interaction extend from a binding energy of about 1 eV nearly to the Fermi level. Inverse photoemission data for sulfur monolayers on Cu(100) suggest that the corresponding unoccupied S derived levels lie just above the Fermi level.[17] The location of the Fermi level in the midst of this Au−S derived density of states implicates charge transfer associated with S− Au bonding as the controlling factor in Fermi level alignment within the molecular gap for the thiol bound monolayer of OPE.

A simple estimate of the charge transfer, associated with Au−S bonding and necessary to produce the approximately 0.7 eV shift, can be made using

$$\Delta V = N_{\mathrm{mol}} P/2K\epsilon_0$$

where ΔV is the electrostatic potential shift $\approx$0.7 eV, N_{mol} is the number of molecules/m^2 $\approx 4 \times 10^{19}$, P is the dipole per molecule in debye (D), K is the relative dielectric constant $\approx$2 for the monolayer, and ϵ_0 is the permittivity of free space. The measured shift leads to a dipole per molecule of about 1.6 D associated with the Au−S bond. Further assuming a dipole length of about 0.2 nm, the charge transfer is then approximately 0.1 e$^-$, consistent with several theoretical estimates.[15,29,31] This estimate is subject, however, to large uncertainty arising from, among other things, the assumed value of $K \sim 2$ close to the Au interface.

Interest in transport through molecular-scale junctions has stimulated a number of calculations of electronic structure and transmission for related molecular systems, such as benzenethiol[32] and the three-ring oligomer studied in this work.[33] As a case for comparison, we consider the calculations of Taylor et al. that employ a fully atomistic treatment of the electrodes and molecule within density-functional theory (local-density approximation plus gradient corrections). Results were reported for OPE as well as nitro- and amine-substituted molecules.[33,34] For OPE, coupled to two Au electrodes, a peak-to-peak separation of about 2−3 eV is found between the HOMO and LUMO levels, with the Fermi level approximately 1 eV from the HOMO level and ~1.5−2 eV from the LUMO. These values should be compared with measured values in UPS of ~1.9 eV for the separation between E_F and the HOMO and ~3.2 eV from the Fermi level to the LUMO peak. The calculated values for the HOMO−LUMO gap and "injection barriers" are all ~60−100% smaller than experimental findings. The relative location of E_F in the HOMO−LUMO gap compares well between theory and experiment, in both cases giving the ratio (hole injection barrier)/(electron injection barrier) ~ 0.5. Whether or not this is related to the underestimation of the gap inherent in the local-density approximation is unclear. The calculations performed by Taylor et al. employed gradient corrections[33,34] to the local-density approximation, but this is still expected to underestimate the gap.

An alternate comparison of band lineup between experiment and theory employs the benzene e_{1g}-derived level at 3.8 eV. The quasi-localized character of this level on individual rings produces structure that should be reasonably unambiguous to identify in molecular orbital plots and produce narrow line structure in density of states plots, allowing easy comparison between theory and experiment. The calculations for OPE[33] do not extend deep enough in binding energy to access this level, but similar calculations for benzenethiol[34] suggest a binding energy of about 2.4 eV. This is again reduced, by about 60%, from the value of 3.8 eV indicated by UPS for OPE. The agreement appears somewhat better for benzenethiol, but Au substrate d-band interference and perturbations due to Au−S bonding obscure the exact location of this level.

Summary

The occupied and unoccupied electronic levels in the vicinity of the Fermi level have been determined for the conjugated oligomer, 4,4′-(ethynylphenyl)-1-benzenethiol (OPE), on Au. The UPS spectra bear a close resemblance to spectra from analogous conjugated polymers such as PPV. Occupied delo-

calized π levels are located approximately 1.9 eV from E_F, and the corresponding unoccupied π^* levels are estimated to lie about 3.2 eV above E_F. Comparison with representative theory indicates a reasonable agreement for the relative location of the Femi level in the gap between the π and π^* levels, but the values for the gap and the $E_F-\pi$ or $E_F-\pi^*$ separations are ~60−100% larger than calculated. The location of the singlet exciton is determined via two-photon photoemission and is consistent with a polaron−exciton binding energy on the order of 0.7 eV.

Little evidence of the Au−S binding interaction can be observed directly in photoemission spectra from OPE due to limited interaction with the C π levels and localization of the interaction at the molecule−Au interface. Intensity due to Au−S bonding is seen near E_F in companion spectra from monolayers of the shorter benzenethiol molecule. Combined with previous inverse photoemission results, this indicates that the Fermi level is located within the density of states derived from the Au−S interaction. Charge transfer associated with this interaction is suggested to produce the approximately 0.7 eV shift of the Fermi level toward the highest occupied orbitals on the oligomer.

Acknowledgment. The work at Rice University was supported by DARPA and the ONR.

References and Notes

(1) **(1)** Seki, K.; Ishii, H. *J. Electron Spectrosc. Relat. Phenom*. **1998**, *88*, 821. Sugiyama, K.; Yoshimura, D.; Miyamae, T.; Miyazaki, T.; Ishii, H.; Ouchi, Y.; Seki, K. *J. Appl. Phys.* **1998**, *83*, 4928. Kahn, A.; Koch, N.; Gao, W. *J. Polym. Sci. B* **2003**, *41*, 2529.

(2) **(2)** Hill, I. G.; Kahn, A.; Soos, Z. G.; Pascal, R. A., Jr. *Chem. Phys. Lett*. **2000**, *327*, 181.

(3) **(3)** Jacquemin, R.; Kraus, S.; Eberhart, W. *Solid State Commun*. **1998**, *105*, 449. Link, S.; Scholl, A.; Jacquemin, R.; Eberhart, W. *Solid State. Commun*. **2000**, *113*, 689. Link, S.; Durr, H. A.; Eberhart, W. *J. Phys.: Condens. Matter* **2001**, *13*, 7873. Miller, A. D.; Gaffney, K. J.; Liu, S. H.; Szymanski, P.; Garrett-Roe, S.; Wong, C. M.; B Harris, C. *J. Phys. Chem. A* **2002**, *106*, 7636. Vondrak, T.; Wang, H.; Winget, P.; Cramer, C. J.; Zhu, X.-Y. *J. Am. Chem. Soc*. **2000**, *122*, 4700. Dutton, G.; Zhu, X.-Y. *J. Phys. Chem. B* **2002**, *106*, 5975. Zhu, X.-Y. *Annu. Rev. Phys. Chem*. **2002**, *53*, 221.

(4) **(4)** Chen, J.; Reed, M. A.; Rawlett, A. M.; Tour, J. M. *Science* **1999**, *286*, 1550. Chen, J.; Wang, W.; Reed, M. A.; Rawlett, A. M.; Price, D. W.; Tour, J. M. *Appl. Phys. Lett.* **2000**, *77*, 1224.

(5) **(5)** Nitzan, A.; Ratner, M. A. *Science* **2003**, *300*, 1384. Adams, D. M.; et al. *J. Phys. Chem. B* **2003**, *107*, 6668.

(6) **(6)** Greenham, N. C.; Friend, R. H. In *Solid State Physics*; Ehrenreich, H., Spaepen, F., Eds.; Academic Press: New York, 1995; Vol. 49. Salaneck, W. R.; Stafstrom, S.; Bredas, J.-L. *Conjugated Polymer Surfaces and Interfaces*; Cambridge University Press: Cambridge, 1996; p 51 ff.

(7) Tour, J. M. *Molecular Electronics: Commercial Insights, Chemistry, Devices, Architecture and Programming:* World Scientific: Teaneck, NJ, 2003.

(8) Certain commercial equipment, instruments, or materials are identified in this paper to foster understanding. Such identification does not imply recommendation or endorsement by the National Institute of Standards and Technology, nor does it imply that the materials or equipment identified are necessarily the best available for this purpose.

(9) Zangmeister, C. D.; Robey, S. W.; van Zee, R. D., unpublished results.

(10) Asbrink, L.; Edqvist, O.; Lindholm, E.; Sedin, L. E. *Chem. Phys. Lett*. **1972**, *5*, 192. Lindholm, E.; Asbrink, L. *Molecular Orbitals and Their Energies Studied by the Semiempirical HAM Method*; Lecture Notes in Chemistry; Berthier, G., Ed.; Springer: Berlin, 1985.

(11) Dudde, R.; Frank, K.-H.; Koch, E.-E. *Surf. Sci*. **1990**, *225*, 267.

(12) Duke, C. B.; Salaneck, W. R.; Fabish, T. J.; Ritsko, J. J.; Thomas, H. R.; Patton, A. *Phys. Rev. B* **1978**, *18*, 5717.

(13) Fahlman, M.; Logdlund, M.; Stafstrom, S.; Salaneck, W. R.; Friend, R. H.; Burn, P. L.; Holmes, A. B.; Kaeriyama, H.; Sonoda, Y.; Lhost, O.; Meyers, F.; Bredas, J.-L. *Macromolecules* **1995**, *28*, 1959. Salaneck, W. R.; Stafstrom, S.; Bredas, J.-L. *Conjugated Polymer Surfaces and Interfaces*; Cambridge University Press: Cambridge, 1996; p 110 ff.

(14) Stapelton, J. J.; Harder, P.; Daniel, T. A.; Reinard, M. D.; Yao, Y.; Price, D. W.; Tour, J. M.; Allara, D. L. *Langmuir* **2003**, *119*, 8245.

(15) Xue, Y.; Datta, A. S.; Ratner, M. A. *J. Chem. Phys*. **2001**, *115*, 4292.

(16) Argon, P. A.; Carlson, T. A. *J. Vac. Sci. Technol*. **1982**, *20*, 815. Shen, W.; Nyberg, G. L.; Liesegang, J. *Surf. Sci*. **1993**, *298*, 143. Argon, P. A.; Carlson, T. A.; Dress, W. B.; Nyberg, G. L. *J. Electron Spectrosc. Relat. Phenom*. **1987**, *42*, 313. Whelan, C. M.; Barnes, C. J.; Walker, C. G. H.; Brown, N. M. D. *Surf. Sci*. **1999**, *425*, 195. Abduanni, A.; Kera, S.; Aoki, M.; Okudaira, K. K.; Ueno, N.; Harada, Y. *J. Electron Spectrosc. Relat. Phenom*. **1998**, *88*, 849.

(17) Leschik, G.; Couths, R.; Wern, H. *Surf. Sci*. **1993**, *294*, 355.

(18) Alloway, D. M.; Hofmann, M.; Smith, D. L.; Gruhn, N. E.; Graham, A. L.; Colorado, R.; Wysocki, V. H.; Lee, T. R.; Lee, P. A.; Armstrong, N. R. *J. Phys. Chem. B* **2003**, *107*, 11690.

(19) Felice, R. D.; Selloni, A.; Molinari, E. *J. Phys. Chem. B* **2003**, *107*, 1151.

(20) Zangmeister, C. D.; Robey, S. W.; van Zee, R. D. *J. Am. Chem. Soc*. **2004**, *126*, 3420.

(21) Velic, D.; Hotzel, A.; Wolf, M.; Ertl, G. *J. Chem. Phys*. **1998**, *109*, 9155.

(22) Dhirani, A.; Lin, P.-H.; Guyot-Sionnest, P.; Zehner, R. W.; Sita, L. R. *J. Chem. Phys*. **1997**, *106*, 5249.

(23) Frank, K.-H.; Dudde, R.; Koch, E. E. *Chem. Phys. Lett*. **1986**, *132*, 83.

(24) Ray, K.; Shanzer, A.; Waldeck, D. H.; Naaman, R. *Phys. Rev. B* **1999**, *60*, 13347. Naaman, R.; Vager, Z. *Acc. Chem. Res.* **2003**, *36*, 291.

(25) Heurich, J.; Cuevas, J. C.; Wenzel, W.; Schon, G. *Phys. Rev. Lett*. **2002**, *88*, 256803.

(26) Knupfer, M. *Appl. Phys. A* **2003**, *77*, 623.

(27) Loglund, M.; Salaneck, W. R.; Meyers, F.; Bredas, J.-L.; Arbuckle, G. A.; Friend, R. H.; Holmes, A. B.; Froyer, G. *Macromolecules* **1993**, *26*, 3815. Sato, N.; Loglund, M.; Lazzaroni, R.; Bredas, J.-L.; Bradley, D. D. C.; Friend, R. H.; Ziemelis, K. E. *Chem. Phys.* **1992**, *160*, 299.

(28) Yannoulis, P.; Frank, K.-H.; Koch, E.-E. *Surf. Sci*. **1991**, *241*, 325.

(29) Piccinin, S.; Selloni, A.; Scandolo, S.; Scoles, G. *J. Chem. Phys.* **2003**, *119*, 6729.

(30) Tomfohr, J. K.; Sankey, O. F. *Phys. Rev. B* **2002**, *65*, 245105.

(31) Majumder, C.; Briere, T.; Mizuseki, H.; Kawazoe, Y. *J. Chem. Phys*. **2002**, *117*, 7669.

(32) Lang, N. D.; Avouris, Ph. *Phys. Rev. B* **2001**, *64*, 125323. Ventra, M. D. Pantelides, S. T.; Lang, N. D. *Phys. Rev. Lett.* **2000**, *84*, 979. Emberly, E. G.; Kirczenow, G. *Phys. Rev. B* **1998**, *58*, 10911. Magoga, M.; Joachim, C. *Phys. Rev. B* **1997**, *56*, 4722. Xue, Y.; Datta, S.; Ratner, M. A. *J. Chem. Phys*. **2001**, *115*, 4292.

(33) Kaun, C.-C.; Larade, B.; Guo, H. *Phys. Rev. B.* **2003**, *67*, 121411. Taylor, J.; Brandbyge, M.; Stokbro, K. *Phys. Rev. Lett.* **2002**, *89*, 138301. Stokbro, K.; Taylor, J.; Brandbyge, M. *J. Am. Chem. Soc*. **2003**, *125*, 3674. Taylor, J.; Brandbyge, M.; Stokbro, K. *Phys. Rev. B* **2003**, *68*, 121101.

(34) Stokbro, K.; Taylor, J.; Brandbyge, M.; Mozos, J.-L.; Ordejon, P. *Comput. Mater. Sci.* **2003**, *27*, 151.